Hydrodynamic Focusing on a Silicon Chip: Mixing Nanoliters in Microseconds

James B. Knight, Ashvin Vishwanath, James P. Brody, and Robert H. Austin
Department of Physics, Princeton University, Princeton, New Jersey 08544
(Received 4 November 1997)

We describe the formation and control of nanoscale, submerged fluid jets. The focusing process necessary to achieve these small length scales is characterized experimentally and theoretically. Fast mixing is one important application of nanoscale fluid control: We demonstrate this with a continuous-flow mixer capable of mix times of less than 10 μs and sample consumption rates of nanoliters per second. This new technique facilitates the study of fast reaction kinetics on time scales unattainable with conventional mixing technology. [S0031-9007(98)05809-8]

PACS numbers: 47.60.+i, 07.10.Cm, 47.27.Wg, 87.80.+s

Mixing is driven by diffusion, and is therefore slow over macroscopic length scales. It is frustrating, for example, to wait passively for cream to mix evenly into a cup of coffee. More seriously, many liquid-phase chemical and biological processes exhibit dynamics that cannot be resolved in reaction kinetics experiments because they are faster than the mix times of conventional mixers [1]. Protein folding is one important example in which the current emphasis is on time scales shorter than the millisecond mixing times attainable with traditional, stopped-flow methods [2].

Diffusion can be enhanced by turbulence to accelerate mixing, as when coffee and cream are stirred with a spoon. Similarly, the fastest mixers used for reaction kinetics introduce turbulence by forcing reactant streams at high velocity through a nozzle. This technique can yield mix times below 100 μs, but it is inherently difficult to control and consumes large volumes of sample [2–5]. The transit time of the mixed fluid through the nozzle further imposes a dead time during which the reaction is obstructed from view.

A faster alternative to turbulent mixing is to reduce the length scale over which the fluids must diffusively mix: in the parlance of the coffee metaphor, to use a very small cup [6]. We describe in this Letter a microfluidic, continuous-flow mixer capable of diffusive mixing times of less than 10 μs. This is achieved without inducing turbulence and in an open architecture that reduces dead time by permitting observation of the entire mixing process. Figure 1 is an epifluorescence image of the microfabricated device: four rectangular channels, 10 μm deep and wide, intersect at the center. Fluorescent dye labels the flow from the inlet channel and appears bright, while nonfluorescent buffer flows from the side channels. The side flow squeezes, or "hydrodynamically focuses," the inlet flow into a thin stream that exits the intersection sheathed in buffer fluid. The focusing width can be controlled by varying the relative pressures driving the side and inlet flows, and widths as small as 50 nm have been measured. At such small length scales, molecules from the side flow rapidly diffuse across the inlet stream, resulting in fast mixing.

After mixing, the time evolution of any subsequent reaction is separated spatially in the steady-state flow. Time resolution is determined by the flow speed, and the small size of the channels maintains laminar flow even at velocities yielding resolution better than a microsecond per micron. A further consequence of the focusing is the small sample volume consumed by the mixer. The volume flow rates of the focused reactant stream are typically on the scale of nanoliters per second, over 3 orders of magnitude slower than the rates in comparable turbulent mixers [4]. While this renders the technique undesirable for mixing coffee, it is ideal for use with expensive biochemical samples.

The mixers were micromachined on silicon wafers using standard photolithographic techniques and a Cl_2 reactive ion etching process [6,7]. Four channels, rectangular in cross section and etched to a depth of 10 μm, intersect at the center of the mixing chip. Each channel tapers down in width as the channel intersection is approached. The side and outlet channels abutting the intersection are 10 μm wide, while the inlet channel terminates in a 2 μm nozzle.

The chips were sealed on the top with a cover slip coated in a thin layer of cured silicone rubber [7]. The cover slip could be removed after use and the chip cleaned and resealed. Four holes, located at the beginning of each channel, were drilled through the chip prior to sealing [8]. These openings allowed fluid flow into the channels from cylindrical sample reservoirs sealed by o-rings to the back of the chip. Pressure was controlled by regulating a supply of dry nitrogen gas at the head of each tubular reservoir. The pressures reported in this paper correspond to measurements of this pressure head [9].

Fluid flow in the chips was imaged using standard epifluorescence and confocal scanning microscopy [10]. In both cases, the inlet flow was labeled with the fluorescent dye 5-carboxyfluorescein (hereafter referred to as fluorescein). The pH sensitive quantum yield of fluorescein was held constant by buffering at $p\mathrm{H} = 8.5$ with tris-HCl [11]. Average fluid velocity was calculated from the volume rate of flow expelled from the mixer, and was on the order of meters per second at the pressures applied in the experiments described below [12,13].

The focusing region over which the width of the inlet flow rapidly varies extends about one channel width from the inlet opening (see Fig. 1). Once focused, the stream remains of constant width unless broadened by diffusion into the side flow or by an increase in channel width. Flow velocities are held below the threshold for turbulence, and the focused, submerged stream is not subject to the instabilities that can disrupt a macroscopic fluid jet [14].

The width of the focused stream does not depend on the magnitude of the applied pressures, but rather on the ratio α of the side pressure (P_s) to the inlet pressure (P_i): $\alpha = P_s/P_i$. Focusing is observed over a range of α. Below a lower limit $\alpha_{\min}$, fluid from the inlet channel flows out the side channels. Above an upper limit $\alpha_{\max}$, the focused stream is pinched off and fluid from the side channels flows out the inlet channel. Both $\alpha_{\min}$ and $\alpha_{\max}$ are independent of the overall pressure scale, but are dependent upon the details of channel geometry. In the chip shown in Fig. 1, the measured values are $\alpha_{\min} = 0.48 \pm 0.01$ and $\alpha_{\max} = 1.28 \pm 0.01$.

The three-dimensional structure of hydrodynamic focusing is shown in Fig. 2. Confocal scanning microscopy was used to image flow at several values of α. The fluorescein labeling the inlet flow is bright in the image, while the surrounding fluid and the channel walls are not. The view is oriented such that the fluorescein is moving diagonally from left to right towards the reader. As α is increased, the focused stream narrows. At $\alpha = 0.5$, some diffusive broadening of the flow is apparent near the top and bottom of the channel, where velocities are lowest.

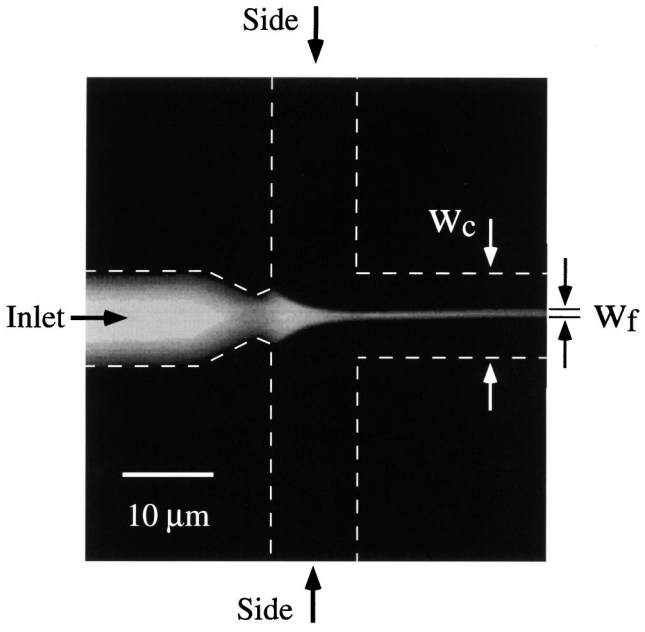

FIG. 1. Hydrodynamic focusing with $P_i = 5$ psi and $\alpha = 1.1$. The edges of the channels are outlined with a dashed line for reference. The variables w_c and w_f describe the width of the channel (10 μm) and the width of the focused inlet stream.

In the faster flows at higher α, this is not a factor, and the cross section of the focused stream appears rectangular. The width of the focused stream is therefore a well-defined quantity.

Many aspects of hydrodynamic focusing are described by a simple circuit model. The fluid flow can be mapped to a network of resistors, provided two conditions hold: The flow must be laminar, and the width of the intersection negligible compared to the length of the channels [15]. Both of these conditions are satisfied in the mixer described here, and the corresponding circuit is shown in the inset of Fig. 3. The pressure and the volume flow rate map to the electric potential and current. The relationship between fluid flux and pressure is a hydrodynamic analog to Ohm's law from which the appropriate resistance can be calculated from channel geometry. The inlet branch of the circuit is driven by voltage V_i and the sides by αV_i. The outlet branch terminates at ground. The resistances of the side, inlet, and outlet arms of the circuit are R, γR, and σR, respectively, with the parameters γ and σ reflecting differences in channel geometry.

The pattern of current flow shown in the diagram corresponds to focusing and occurs in the range $\alpha_{\min} < \alpha < \alpha_{\max}$. The limiting values are a function of the resistance in each circuit arm: $\alpha_{\max} = (1 + 2\sigma)/2\sigma$ and $\alpha_{\min} = \sigma/(\sigma + \gamma)$. The parameters $\sigma = 1.73$ and $\gamma = 1.78$ were calculated for the mixing chip using the analytical expression for the volume flow rate in a rectangular channel [13]. The resulting values of $\alpha_{\min} = 0.49$ and $\alpha_{\max} = 1.29$ are in excellent agreement with the experimental values of $\alpha_{\min} = 0.48 \pm 0.01$ and $\alpha_{\max} = 1.28 \pm 0.01$.

Measurements of the width of the focused inlet stream on the micron scale or larger can be obtained directly from microscope images, such as Fig. 1, but the accurate determination of smaller focusing widths requires a

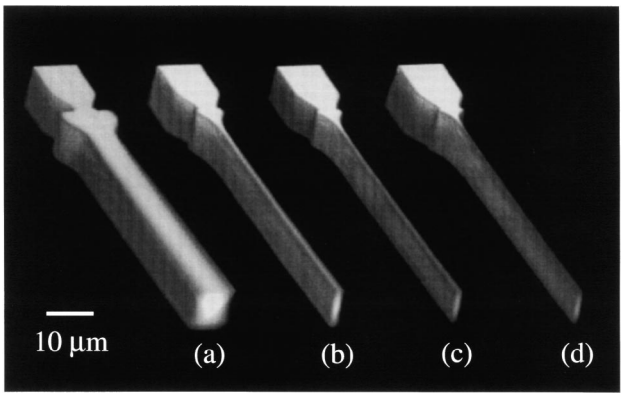

FIG. 2. Confocal scanning microscopy images of hydrodynamic focusing with $P_i = 5$ psi and (a) $\alpha = 0.5$, (b) 1.0, (c) 1.1, and (d) 1.2. Fluorescein was used to label the inlet flow and appears bright. Each three-dimensional rendering is formed from approximately 30 separate two-dimensional images acquired at regular intervals in depth.

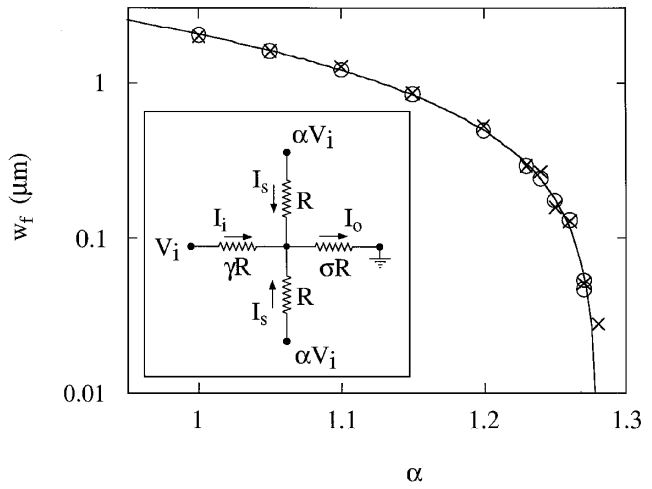

FIG. 3. The width of the focused inlet stream plotted on a logarithmic scale against α. The inlet pressure was held constant at $P_i = 10$ psi. Data from two separate experiments ($\times$ and $\bigcirc$) are shown and agree within experimental error. The solid line is a one parameter, least-squares fit to Eq. (2) with $B = 1.6$. The inset is a diagram of the resistive circuit corresponding to fluid flow in the mixer.

nonimaging approach. Therefore, a fluorescence technique was used to accurately measure the tightest focusing. The intensity of fluorescent light emitted per unit length from an inlet stream focused to an unknown width was compared with that from a channel of known dimensions filled with the same solution. With constant fluorophore density and a rectangular focusing cross section (Fig. 2), the ratio of the intensities is proportional to the ratio of the widths. Figure 3 is a plot of focused width against α obtained with this technique. The smallest measured focusing widths are less than 50 nm. The reproducible formation of smaller jets was limited by the finite precision with which the pressure (and therefore α) could be controlled.

The solid line in Fig. 3 is a least-squares fit to a functional form calculated from the circuit mapping. The ratio of the inlet current to the outlet current in the circuit is proportional to the ratio of the inlet fluid flux to the outlet flux in the mixer. Together with the assumption of a rectangular focusing cross section, this yields an expression for the focusing width [16]:

$$\frac{w_f}{w_c} = B\,\frac{(1 + 2\sigma - 2\sigma\alpha)}{(1 + 2\sigma\gamma\alpha)}, \qquad (1)$$

where B is a constant of order 1 dependent on channel geometry, and w_c is the width of the outlet channel. Only B was allowed to vary in the fit of Fig. 3; σ and γ were fixed by the experimentally measured values of $\alpha_{\min}$ and $\alpha_{\max}$.

The focusing ratio w_f/w_c at a given value of α is the key performance indicator for diffusive mixing, and the circuit model of the fluid flow outlines a straightforward means of improving it. Equation (1) indicates that tighter focusing can be achieved by increasing γ, the ratio of the inlet resistance to the side resistance. It can also be shown that increasing γ reduces the sensitivity of the width to changes in α near $\alpha_{\max}$, thereby improving the precision with which the focusing width can be experimentally controlled. Applying these insights, we constructed a second mixer with a higher value of γ that performed as predicted and exhibited tighter focusing [15,17].

Fast mixing was observed directly with a diffusion-controlled fluorescence quenching reaction [3]. An inlet flow of fluorescein was focused by a side flow containing iodide (I^-) ions [18]. Iodide ions "quench" light emission by providing a nonfluorescent pathway through which excited fluorescein molecules can relax to their ground state. The rate-limiting step of this reaction is the diffusion of iodide ions to the fluorescein molecules, ideally suiting iodide quenching to measurements of mixing. The fluorescence quantum yield of a fluorescein and I^- mixture depends strongly upon the concentration of I^-, and the time evolution of the I^- diffusion into the fluorescein was detectable as a change in the fluorescence intensity [19].

Figure 4 shows an example of mixing data obtained with this technique. The details of this measurement are reported elsewhere [15]. The mixing fraction was calculated from fluorescence emission and is defined to vary between 0 and 1 as the reactants mix, with 1 representing complete mixing. In Fig. 4, the mixing proceeds rapidly and is essentially complete after 20 μs. We quantified this mixing time by fitting the data to a functional form derived from the diffusion equation.

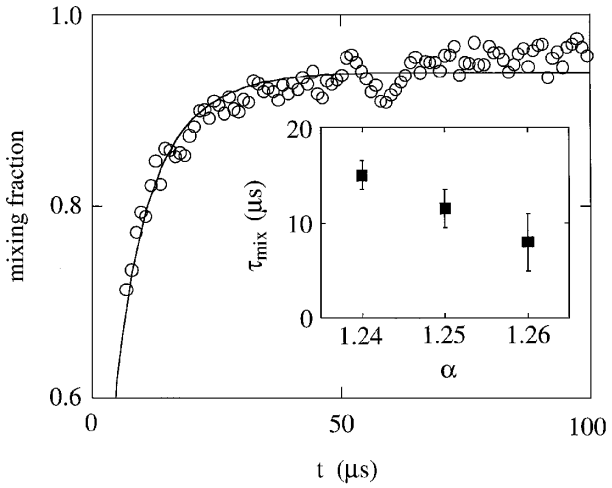

FIG. 4. The mixing fraction as a function of time for $P_i = 40$ psi and $\alpha = 1.25$. Reaction time t was calculated by dividing the distance along the focused stream from the point of initial focus by the flow velocity. The solid line is a best fit to a functional form calculated for diffusion into a rectangular cross section. The inset shows the mix times determined from similar fits to mixing data obtained for several values of P_i and α.

The time dependence is approximately exponential, with a time constant τ_{mix} dependent upon jet width and the diffusion of iodide (D): $\tau_{\text{mix}} = (w_f^2/\pi^2 D)$ [15]. The inset of Fig. 4 shows τ_{mix} determined from these fits for several values of the inlet pressure and the focusing parameter α. Mix times below 10 μs are easily attained and reproducible, and the trend of the mix times is consistent with τ_{mix} going to zero as α_{max} is approached.

Mix times for $\alpha > 1.26$ could not be resolved due to optical limitations, yielding an effective dead time in this experiment of approximately 5 μs. This is to be compared to a typical dead time of 80 μs or more in turbulent mixers [3]. Furthermore, some mixing can also occur along the edges of the inlet flow in the transition region before focusing is complete. The fit to the data in Fig. 4, extrapolated to $t = 0$, indicates that about 5% of the mixing occurred prior to the position along the focused stream that was defined as the origin in time, yielding an additional effective dead time on the order of a microsecond. Similar measurements over several values of the inlet pressure demonstrate that this "premixing" increases with α, but diminishes as the overall speed of the flow is increased [15].

In addition to lowering the mix time, hydrodynamic focusing also dramatically reduces the volume of sample necessary for continuous flow reaction kinetics experiments. In the experiments which generated Fig. 4, the estimated flow rate from the inlet channel was approximately 5 nℓ per second. This is to be compared with flow rates of approximately 10 $\mu\ell$ per second in turbulent mixers [4]. A cumulative 5 s of data acquisition was needed to acquire the necessary images, consuming 25 nℓ of solution from the inlet channel and 1 $\mu\ell$ from the side channels. This frugality makes continuous-flow reaction kinetics experiments a practical alternative for even the costliest samples.

We have described a new approach to continuous-flow reaction kinetics that combines microsecond mix times, nanoliter sample consumption, and submicrosecond time resolution. This is achieved without resorting to turbulent flow, and with the entire mixing process open to view. The hydrodynamic focusing necessary to accomplish this has been experimentally characterized, and a simple model both explains the data and suggests a means of improving performance even further. Reducing the width of the inlet channel enhances focusing, suggesting the use of nanofabrication techniques to push microfluidics into even smaller length scales.

We thank R. Carlson, W. Eaton, J. Hofrichter, A. Madhav, P. Mucha, and L. Sohn for enlightening discussions; B. Dix, J. Goodhouse, B. Gibbs, and the staff of the Cornell Nanofabrication Facility for technical support; and the Princeton Materials Institute and the Robert H. Dicke Foundation for funding.

[1] H. Strehlow, *Rapid Reactions in Solution* (VCH Publishers, New York, 1992).
[2] For a review, see William A. Eaton *et al.,* Structure **4**, 1133 (1996).
[3] C.-K. Chan *et al.,* Proc. Natl. Acad. Sci. U.S.A **94**, 1779 (1997).
[4] S. Takahashi *et al.,* J. Biol. Chem. **270**, 8405 (1995).
[5] P. Regenfuss *et al.,* Rev. Sci. Instrum. **56**, 283 (1985); S. F. Simpson, J. R. Kincaid, and F. J. Holler, Anal. Chem. **55**, 1420 (1983); P. Davidivits and S.-C. Chao, Anal. Chem. **52**, 2435 (1980); G. W. Moscowitz and R. L. Bowman, Science **153**, 428 (1966).
[6] J. P. Brody *et al.,* Biophys. J. **71**, 3430 (1996).
[7] RTV 615 silicone rubber compound, GE Silicones, Waterford, NY; see R. H. Carlson *et al.,* Phys. Rev. Lett. **79**, 2149 (1997); R. H. Carlson, Ph.D. dissertation, Princeton University, 1997.
[8] The silicon chips were affixed with wax (glycol pthylate) to an aluminum base before drilling. This stabilized the chip and reduced chipping and cracking. The holes were drilled at high speeds (14 000 rpm) in water with 0.032 in. diamond mandrils (Lucas Abrasives).
[9] The sample reservoirs contribute a negligible amount to the pressure drop due to their comparatively large radii.
[10] Standard epifluorescence images were captured with a Hammamatsu C4880 cooled CCD camera. The confocal images were collected with a Bio-rad MRC600 Laser Scanning Microscope with an argon/krypton mixed gas laser.
[11] See R. P. Haugland, *Handbook of Fluorescent Probes and Research Chemicals* (Molecular Probes, Inc., Eugene, OR, 1997).
[12] The average flow velocity V_{avg} in the outlet channel was measured to be $V_{\text{avg}} = \beta P_s$, with $\beta = (3.46 \pm 0.03 \times 10^4$ (μm/s)/psi. The focused stream lies in the center of the outlet channel, and the ratio of the central channel velocity V_c (averaged over depth) to the average channel velocity was calculated for laminar flow in a rectangular channel: $V_c/V_{\text{avg}} \approx 1.5$ (see Ref. [13]).
[13] V. N. Constantinescu, *Laminar Viscous Flow* (Springer-Verlag, New York, 1995).
[14] J. A. Roberson and C. T. Crowe, *Engineering Fluid Dynamics* (Wiley, New York, 1993); G. K. Batchelor, *An Introduction to Fluid Dynamics* (Cambridge University, Cambridge, England, 1967).
[15] J. B. Knight, A. Vishwanath, and R. H. Austin (to be published).
[16] Equation (1) is valid in the limit of $w_f/w_c \ll 1$.
[17] A second mixer design was constructed with a 4 μm inlet channel and 40 μm side and outlet channels, resulting in $\sigma = 1.47$ and $\gamma = 5.28$.
[18] The inlet flow was composed of 50 μM 5-carboxyfluorescein in 50 mM tris-Cl buffer (pH 8.5). The side flow was composed of 125 mM NaI in 50 mM tris-Cl buffer (pH 8.5).
[19] K. A. Connors, *Chemical Kinetics: The Study of Reaction Rates in Solution* (VCH Publishers, New York, 1990).